Inelastic Light scattering and the correlated metal-insulator transition

Jim Freericks (Georgetown University)

Tom Devereaux (University of Waterloo)

Ralf Bulla (University of Augsburg)

Funding: National Science Foundation (US)

National Science and Engineering Research Council (Canada)

Deutsche Forschungsgemeinshaft (Germany)

Thanks to: Lance Cooper, Rudi Hackl, Zahid Hasan,

Chuck Irwin, Paul Miller, Z.-X. Shen, and Andrij Shvaika

Raman scattering probes electronic excitations

- **Inelastic scattering of light** with electron-hole excitations of the correlated many-body system.
- Use of polarizers for the incident and reflected light allows one to **select different symmetries** of the electron-hole excitations.
- Signal depends on the **Raman scattering amplitude γ(k)**. We consider three different symmetries here:
- A_{1g}: $\gamma(k) \sim \cos(k_x a)+\cos(k_y a)$
- B_{1g}: $\gamma(k) \sim \cos(k_x a)-\cos(k_y a)$
- B_{2g}: $\gamma(k) \sim \sin(k_x a)\ \sin(k_y a)$

Experimental data for Kondo insulators

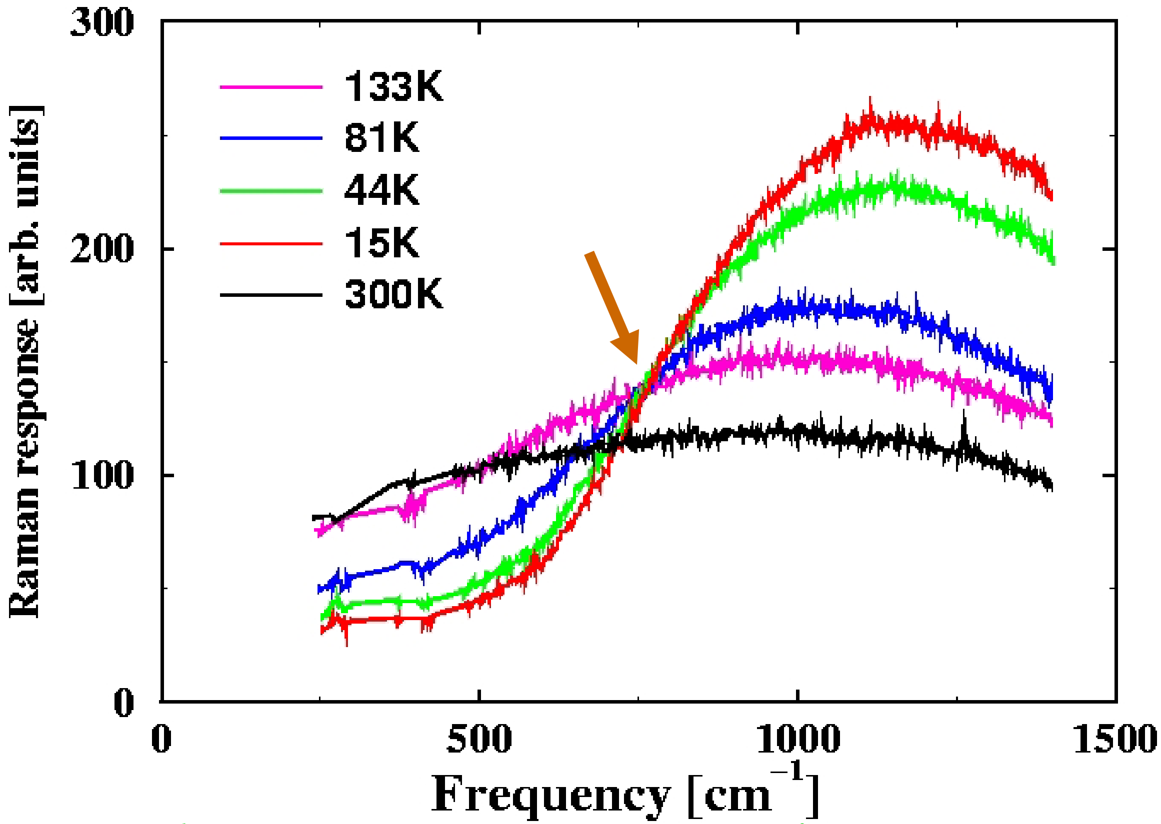

- *Nyhus et al, PRB 95* Raman scattering on **FeSi**. Note the appearance of the **isosbestic point** below about 150K.
- The low frequency spectral weight is **reduced** and the higher frequency weight is **enhanced** as the temperature is lowered.

Experimental data for intermediate-valence materials

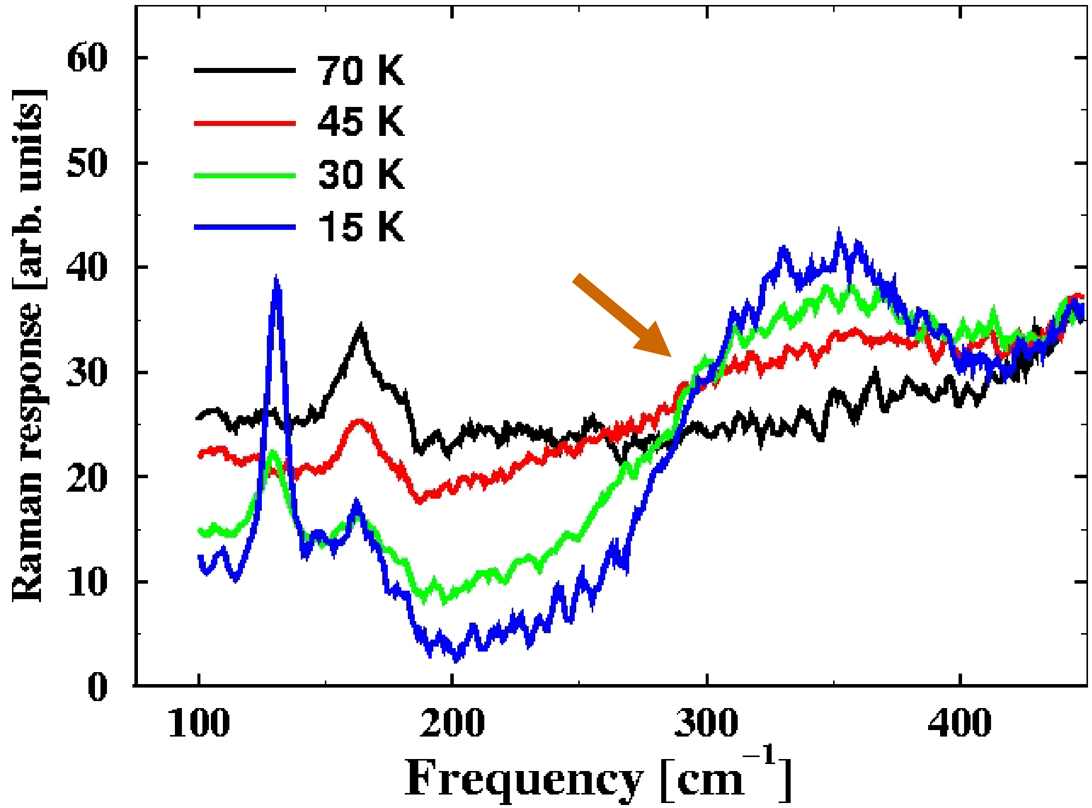

- *Nyhus et al, 1995 and 1997* Raman scattering on **SmB_6**. Note the appearance of the **isosbestic point** near 300 cm^{-1}.
- Below 30K, there is an **increase** in low frequency spectral weight in a narrow peak at about 130 cm^{-1}.

Summary of Experimental Data (Raman)

- Three characteristic behaviors are seen: (i) as T is lowered, there is a **redistribution of spectral weight** from low-frequency to high frequency; (ii) these regions are separated by an isosbestic point, where **the Raman response is independent** of T; (iii) the ratio of the twice spectral range where spectral weight is depleted to the onset temperature, where it first is reduced, is **much larger than 3.5** (typically 10-30).
- For correlated insulators this behavior is **"universal"** in the sense that it **does not depend** on the microscopic properties of the insulating phase, be it a Kondo insulator or an intermediate-valence material.

Resonant **I**nelastic **X**-ray **S**cattering probes momentum and energy dependent charge excitations

- By **tuning** the photon energy to the K or L_3 edge of a core state, one finds large enhancements to the inelastic scattering.
- Advanced light sources have linearly polarized light, but experiments to date have not used polarizers on the detectors. Hence **different symmetry channels are mixed together** in the experimental results.
- The scattered signal depends on the **Raman scattering amplitude $\gamma(\mathbf{k+q/2})$** for transferred momentum **q**.
- The energy resolution in current experiments is poor **(about 0.1ev)** but is expected to improve dramatically with second-generation experiments **(less than 20 meV).**

RIXS on $CaCu_2O_2Cl_2$

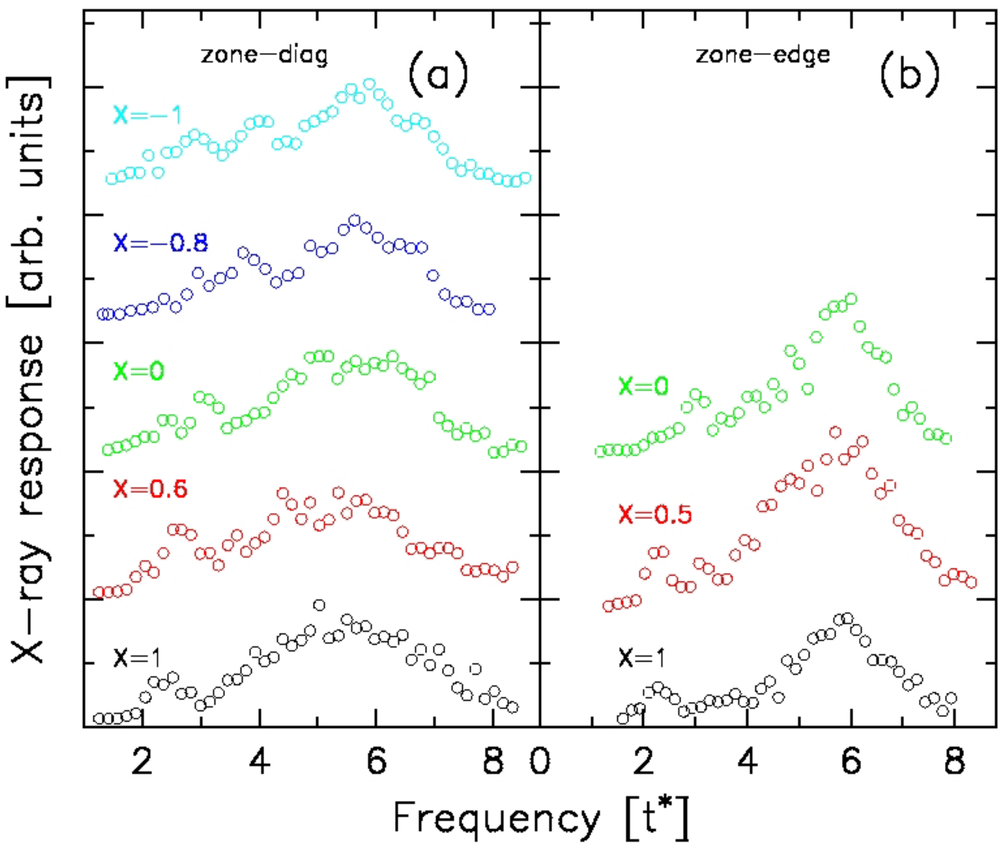

RIXS data from Shen's group, Hasan et al., *Science* 2000.

Experimental data on a Mott insulator shows a **broad charge-transfer peak** and a **dispersive low-energy peak**.

We label the transferred momentum by the parameter $X(\mathbf{q})=[\cos q_x+\cos q_y]/2$. When plotted in this fashion, the dispersion along the zone diagonal and zone center is **similar**.

The difference for X=1 along the different zone axes occurs due to the relation between the polarization vector and **q**, which **differs** for the different directions.

Summary of Experimental Data (RIXS)

- RIXS experiments on correlated insulators typically show two features---(i) a **large-weight charge-transfer peak** and (ii) a **lower-energy peak**. The charge transfer peak shows **little dispersion** through the Brillouin zone, while the lower-energy peak **does disperse**. The dispersion from the zone center to zone corner is usually about **twice** the dispersion from the zone center to the zone edge boundary.
- Experimental results project onto different weights of the different symmetry channels due to a **locking of the photon momentum direction to the polarization of the electric field**.
- Systematic changes in temperature **have not** been carried out yet.

Spinless Falicov-Kimball Model

$$H = -\frac{t}{2\sqrt{d}} \sum_{<i,j>} c_i^\dagger c_j + E \sum_i w_i + U \sum_i c_i^\dagger c_i w_i$$

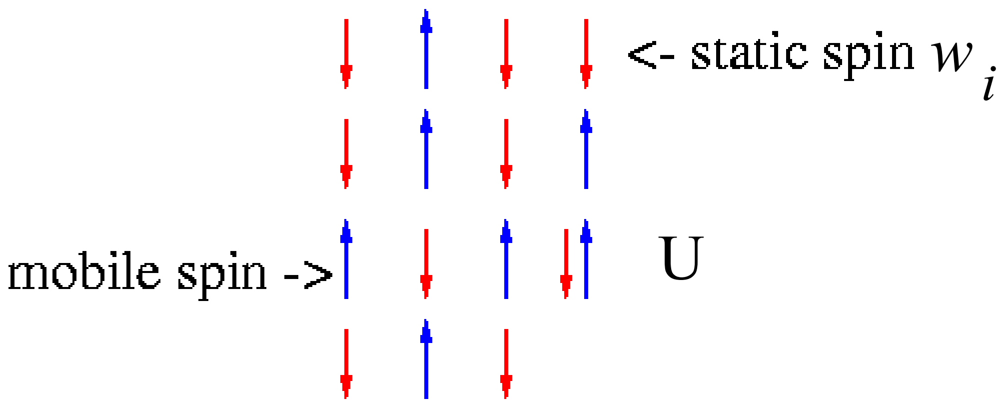

•**exactly solvable model** on a hypercubic lattice in infinite dimensions using dynamical mean field theory.

•possesses homogeneous, commensurate/incommensurate CDW phases, phase segregation, and **metal-insulator transitions**.

•***Raman response can be constructed formally exactly***.

Formal Solution for the Raman Scattering Response A_{1g} channel

- This channel has the **full symmetry** of the lattice
- The Raman response contains **resonant**, **mixed** and **nonresonant** terms. (We consider only the **nonresonant** terms here).
- The irreducible charge vertex for the Falicov-Kimball model is a **simple function** of the electronic self energy and Green's function (Shvaika, Physica C, 2000; Freericks and Miller, PRB, 2000). *This is* ***not*** *true for the Hubbard model*.
- The **nonresonant** Raman response can be determined **exactly** by properly solving the relevant Dyson equations.
- We illustrate how to solve this problem using **Feynman diagrams**.

Diagrams for the A_{1g} Raman response

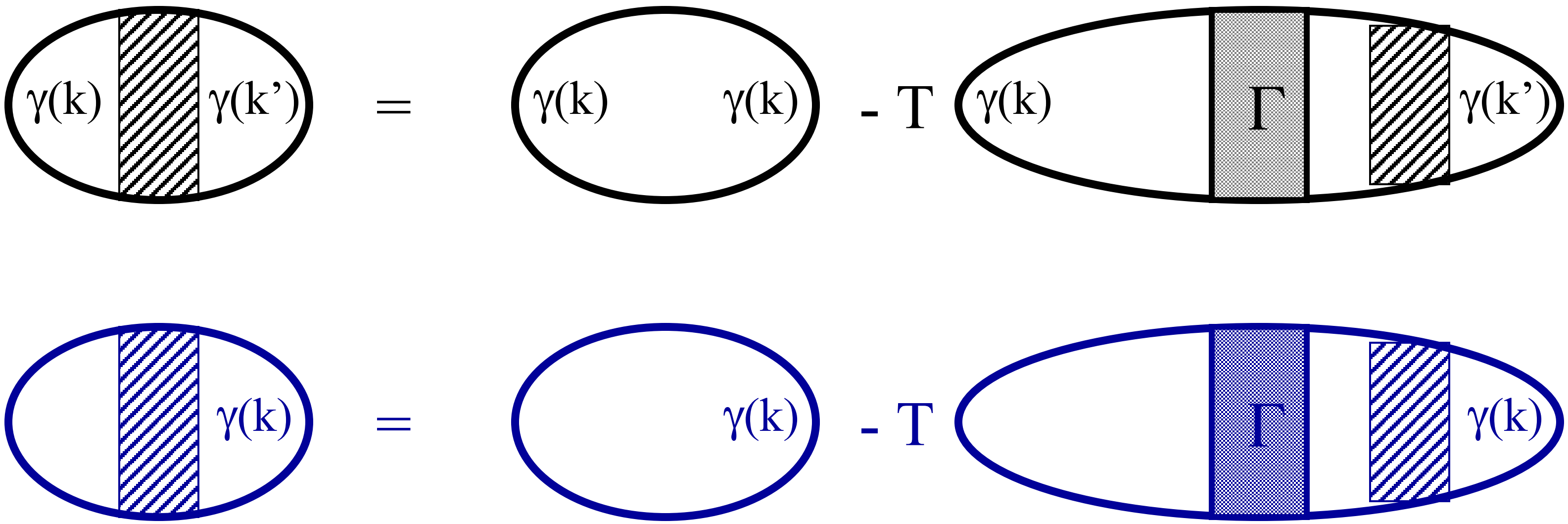

$\gamma(k) = -\varepsilon(k)$, Γ is **local** and has no k-dependence

Solving these coupled equations allows for the full nonresonant Raman response to be determined.

Formal Solution for the Raman Scattering Response
B_{1g} channel

- This channel is **orthogonal** to the lattice.
- There are **no vertex corrections** (Khurana, PRL, 1990), so the Raman response is represented by the **bare bubble**.
- This response is **identical** to that of the optical conductivity multiplied by one factor of frequency (Shastry and Shraiman, PRL, 1990).
- **Resonant** Raman scattering is possible in this channel, but won't be analyzed here.

The nonresonant B_{1g} Raman response is closely related to the optical conductivity.

Formal Solution for Raman the Scattering Response
B_{2g} channel

- The Raman scattering amplitude vanishes for nearest neighbor hopping on a hypercubic lattice, so there are **no nonresonant or mixed responses**.
- The square of the current operator does contain B_{2g} symmetry, so **pure resonant processes are possible**.
- **Vertex corrections** are needed, but are relatively simple to handle.
- We don't discuss this channel further here.

B_{2g} Raman scattering is purely resonant.

Metal-Insulator transition

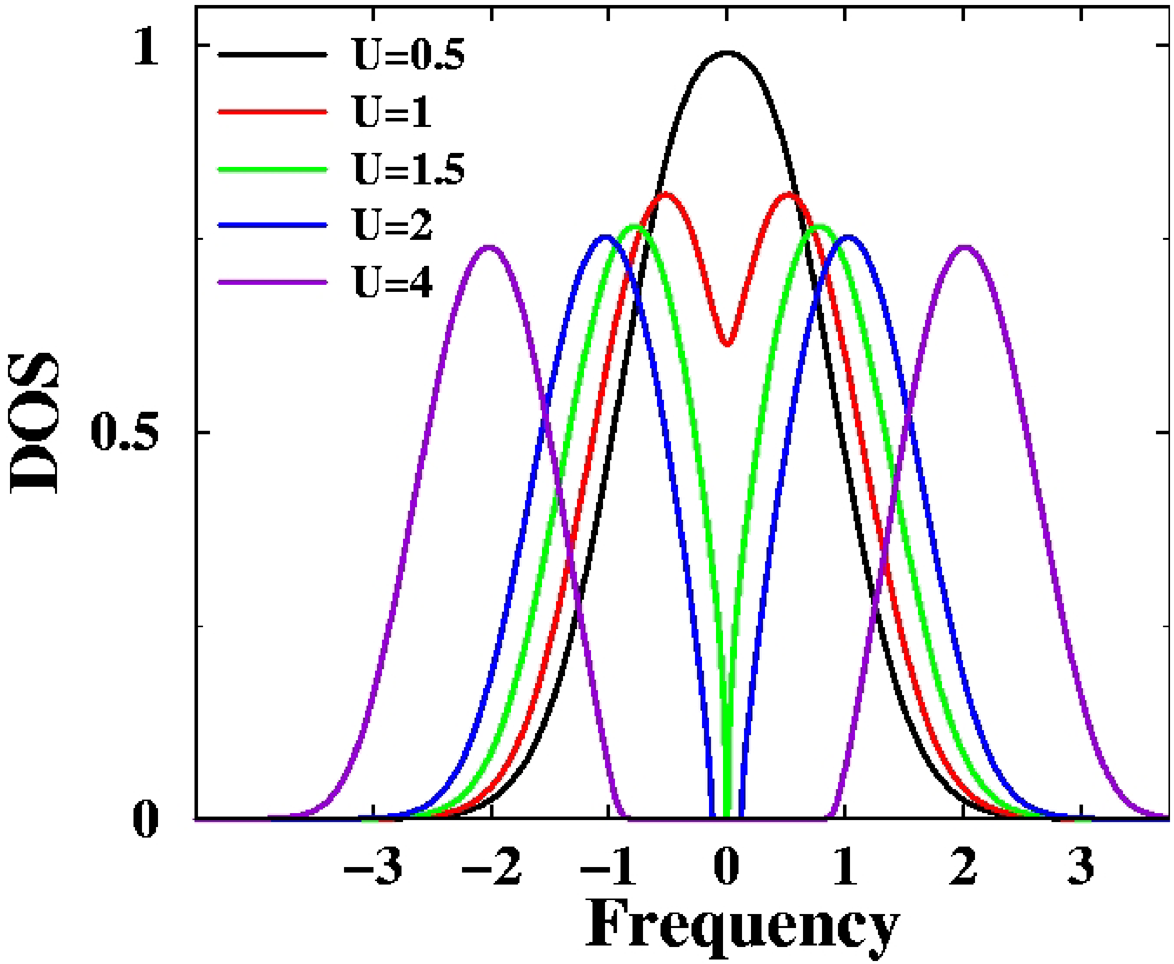

- **Correlation-induced** gap drives the single-particle DOS to zero at U=1.5
- Interacting DOS is **independent of T** in DMFT (Van Dongen, PRB, 1992)
- ***Examine Raman response through the (T=0) quantum phase transition***.

Nonresonant Raman Response (U=2)

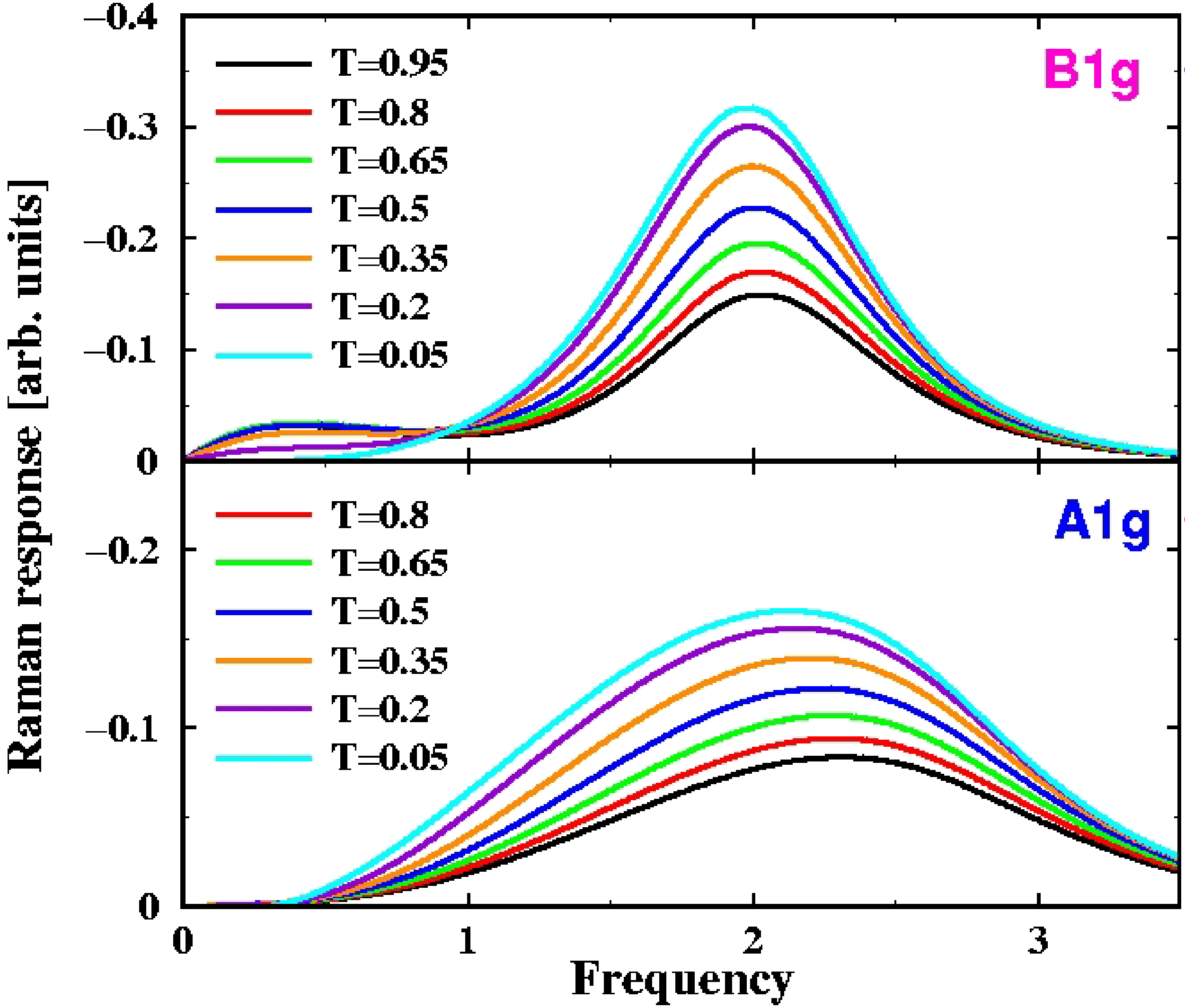

- The low-frequency B_{1g} response develops at a low temperature over a **wide frequency range** of O(1).
- An **isosbestic point** divides where spectral weight increases or decreases as T is lowered (B_{1g}).

Inelastic X-ray scattering (B_{1g})

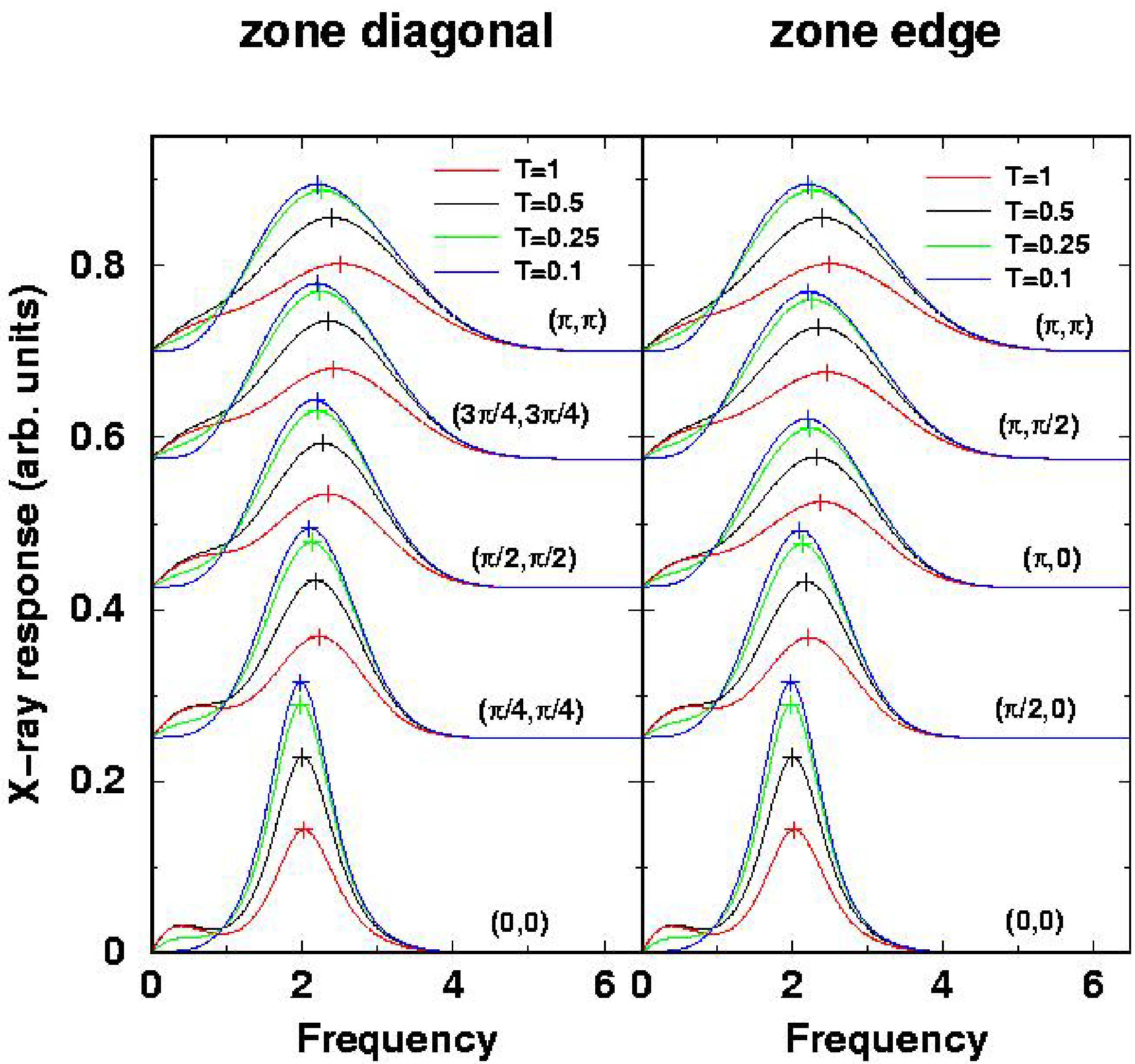

- Scattering of x-rays allows the photon to exchange **both momentum and energy** with the electron-hole excitations.
- We see a **broadening** and **dispersion** of the peaks, but the **same** anomalous low-energy behavior and the isosbestic point.

Inelastic X-ray scattering (A_{1g})

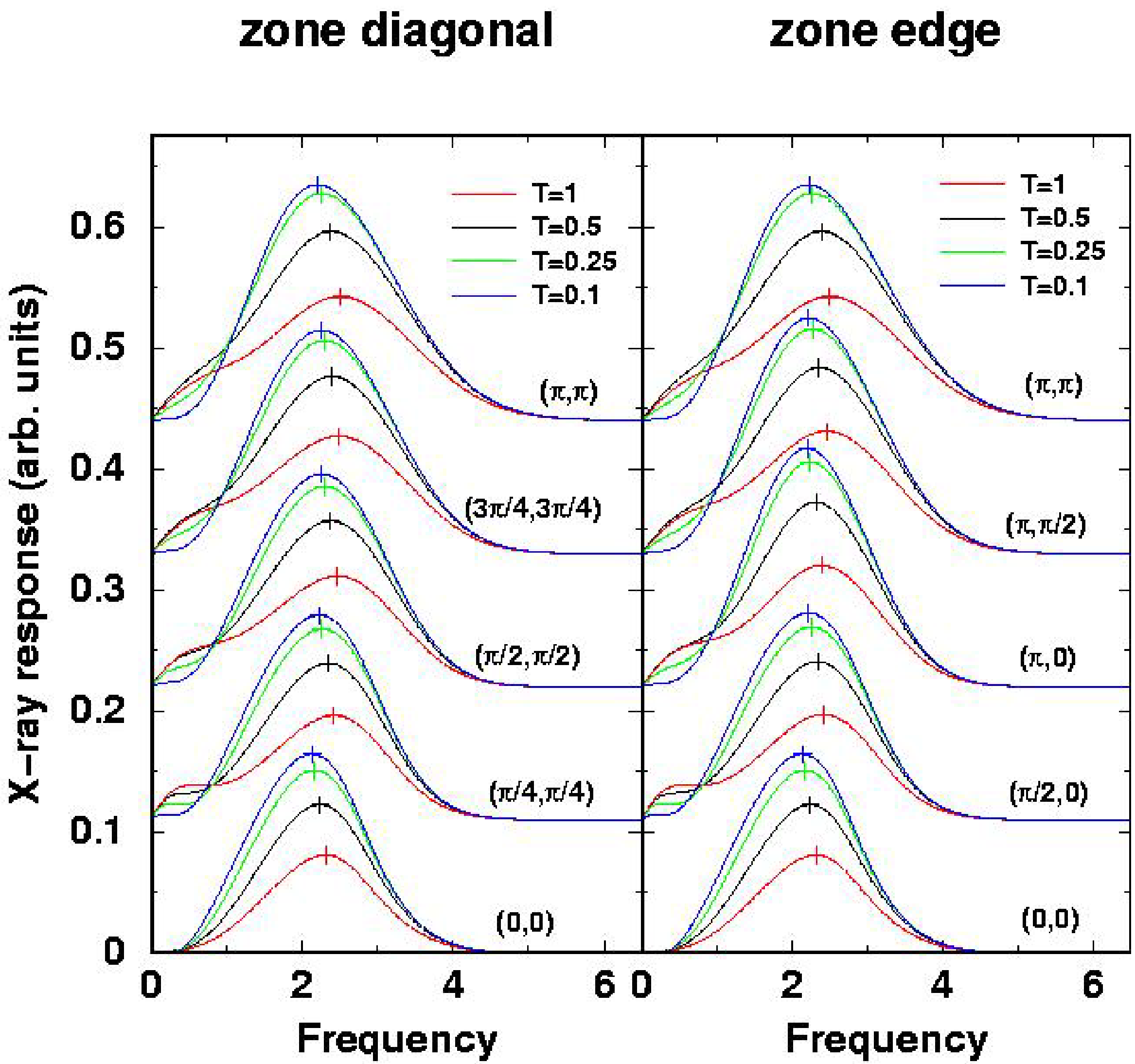

- Here the results at finite-**q** differ greatly from **q**=0: all of the anomalies appear away from **q**=0!
- A reduced **broadening** and **dispersion** of the peaks is seen; but the **same** anomalous low-energy behavior and the isosbestic points recur for nonzero **q**.

Summary (Falicov-Kimball model)

- The theoretical results are **qualitatively similar** to experimental results measured in correlated systems.
- The nonresonant B_{1g} channel displays (i) an **isosbestic point** that divides the regions where the Raman response increase or decrease as T is lowered; (ii) a **sharp depletion of spectral weight** in the low-frequency region as T is reduced; and (iii) the temperature where low-frequency spectral features appear is **much lower than the range** in frequency over which those features appear.
- Results for the Raman scattering are **model independent** on the insulating side of the MIT.
- Vertex corrections **suppress all nontrivial behavior** for the A_{1g} channel at $\mathbf{q}=0$ only.

Hubbard Model

$$H = -\frac{t}{2\sqrt{d}} \sum c^{*}_{i\sigma} \, c_{j\sigma} + U \sum n_{i\uparrow} n_{i\downarrow}$$

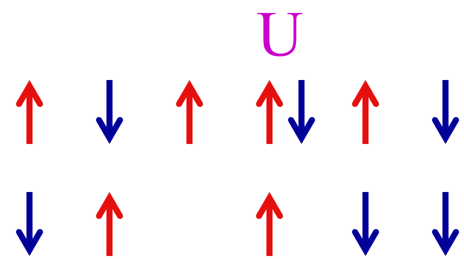

Both electrons are now **mobile**

- **Exactly solvable** model on a hypercubic lattice in infinite dimensions using dynamical mean field theory (but requires **NRG** calculations to extract real frequency information).

- The irreducible charge vertex is **problematic to calculate** because it possesses too large a dynamic range for the max-ent techniques.

- ***Hence, the Raman response can be constructed formally exactly for the nonresonant B_{1g} channel only.***

Nonresonant B_{1g} Raman scattering (n=1,U=2.1)

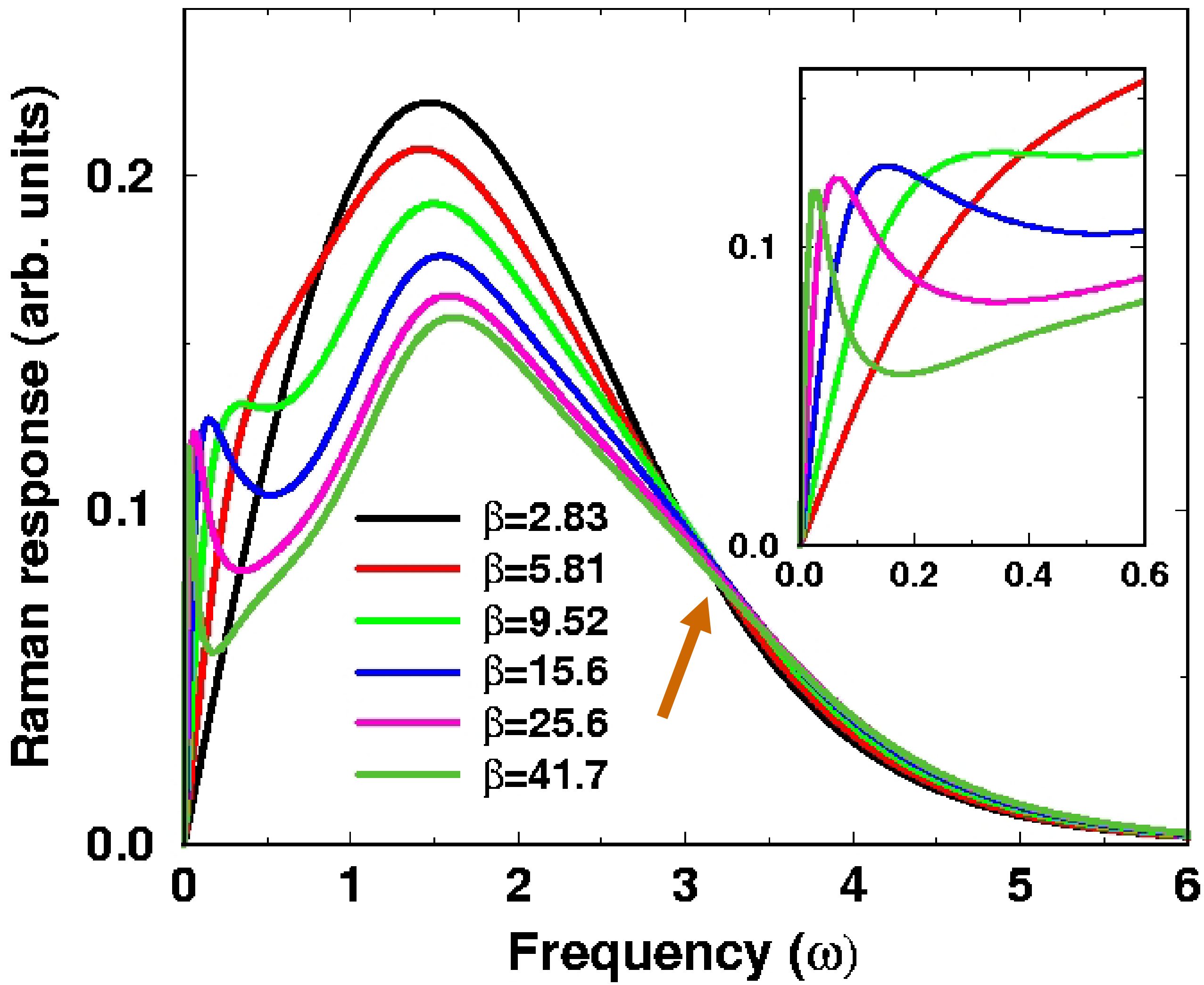

- Note the **charge transfer peak** as well as the **Fermi liquid peak** at low energy. As T goes to zero, the Fermi peak **sharpens** and **moves to lower energy**, as expected.
- There is **no low energy and low-T isosbestic point**, rather a high frequency isosbestic point seems to develop.

Nonresonant B_{1g} Raman scattering (n=1,U=3.5)

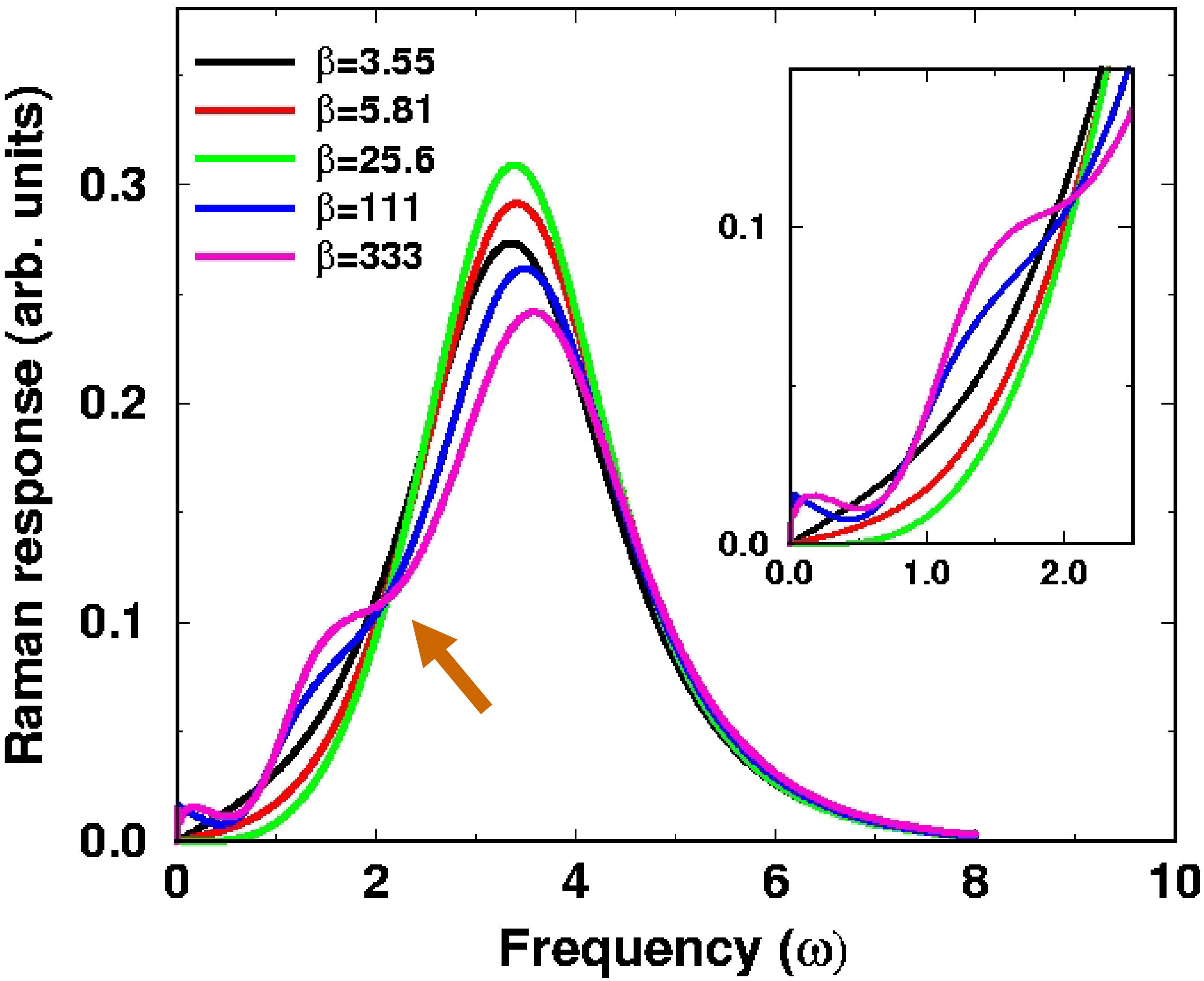

- This is **quite anomalous**! A MIT occurs as a function of T. Note the appearance of the low-T isosbestic point.
- The low energy Raman response has rich behavior, with a number of low energy peaks developing at low-T, but **the low energy weight increases as T decreases here**.

Nonresonant B_{1g} Raman scattering (n=1,U=4.2)

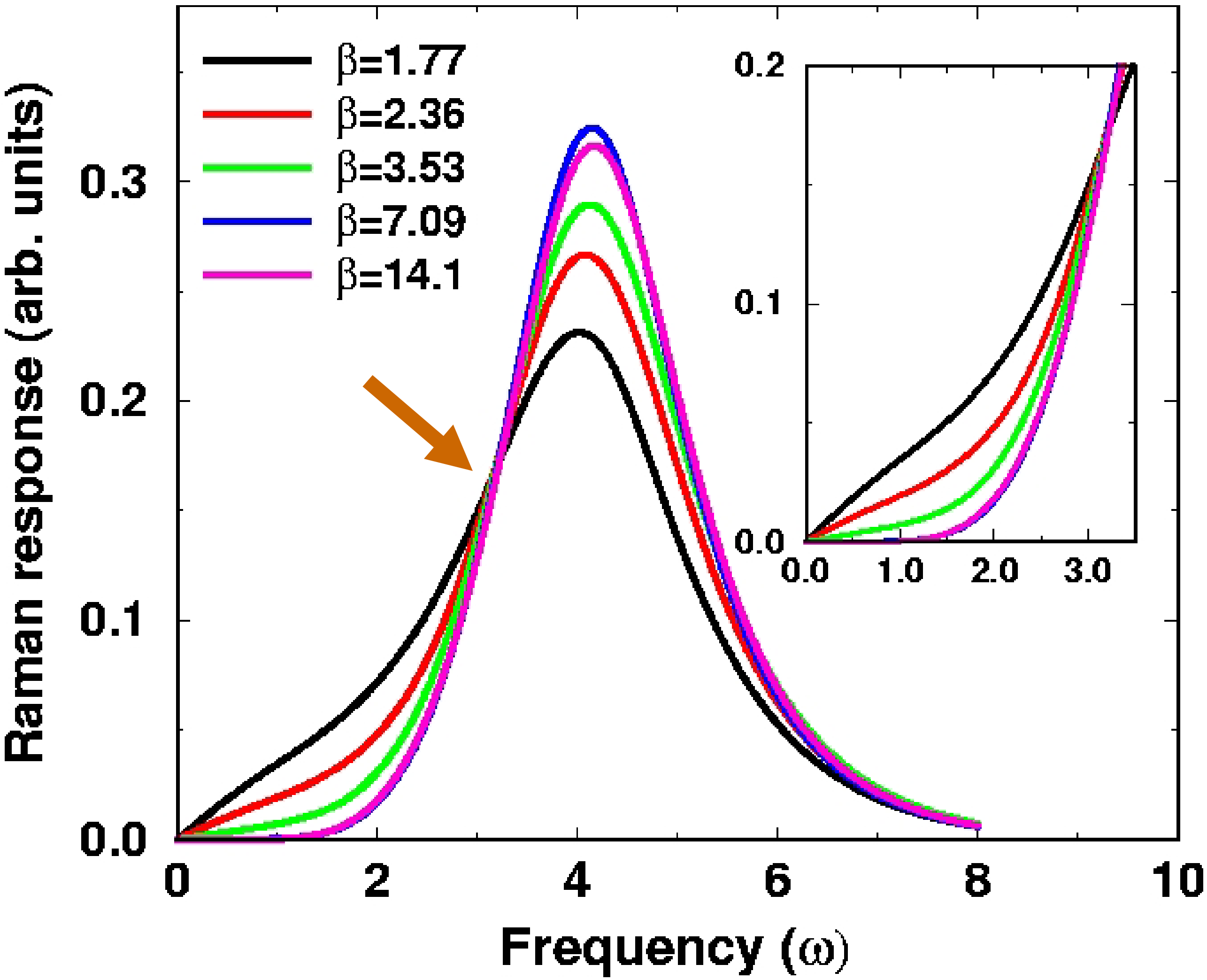

- Here we see the expected **universal behavior** for the insulator---the low-energy spectral weight is **depleted** as T goes to zero and an **isosbestic point** appears.
- The temperature dependence here is over a **wider range** than for the FK model due to the **T-dependence** of the interacting DOS.

Inelastic X-ray scattering (B_{1g}, zone diagonal)

- Nonresonant scattering for a **correlated metal**, a system that undergoes a **metal-insulator transition**, and a **correlated insulator**.
- Note how the Fermi peak **broadens** and **remains away from ω=0** as **q** increases.
- In the MIT case, the scattering results depend **weakly** on T.
- For the insulator, the results are quite similar, except for **some broadening**, as one moves through the Brillouin zone.

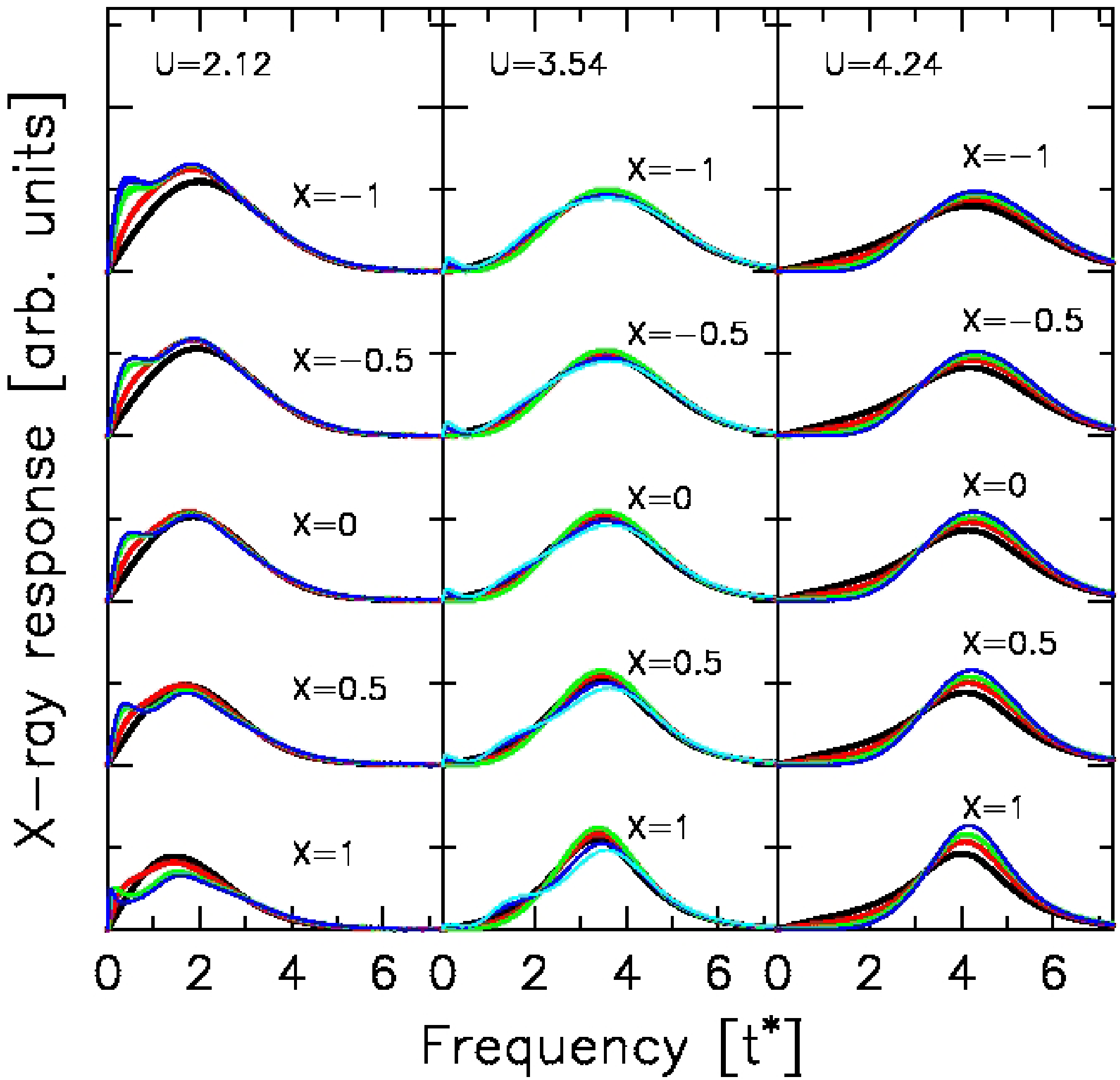

Summary Hubbard model

- The Fermi-liquid behavior introduces new features to the B_{1g} Raman response: there is a characteristic **Drude like feature** that develops at the lowest frequencies (with a width that decreases like T^2).
- New behavior occurs on the metallic side of the MIT, where the **low-energy spectral weight increases** as T decreases and where additional structure is seen, as the system undergoes a temperature-driven insulator-metal transition.
- In the insulating phase we see the expected "**universal behavior**," but the temperature dependence is slower here, because the interacting DOS is also T-dependent.

Conclusions

- Showed how an exact solution for **nonresonant** Raman scattering can be constructed for a system that passes through a metal-insulator transition. The solutions displayed both an **isosbestic point** and a **rapid increase in low-frequency spectral weight** near the quantum-critical point, just as seen in experiment.
- Results are **model independent** or **“universal”** on the insulating side of the metal-insulator transition, explaining why so many different correlated insulators show similar behavior.
- Found the presence of **a low frequency Drude peak** in the Fermi-liquid metals.
- Showed interesting universal features are to be expected with **inelastic x-ray scattering** as well.